JPE 16-5-6

http://dx.doi.org/10.6113/JPE.2016.16.5.1678
ISSN(Print): 1598-2092 / ISSN(Online): 2093-4718

Design of Capacitive Power Transfer Using a Class-E Resonant Inverter

Yusmarnita Yusop*, Shakir Saat†, Sing Kiong Nguang**, Huzaimah Husin*, and Zamre Ghani*

*,†Advance Sensors & Embedded Control System (ASECS) Research Group, Faculty of Electronics & Computer Engineering, Universiti Teknikal Malaysia Melaka, Melaka, Malaysia
**Department of Electrical & Computer Engineering, The University of Auckland, Auckland, New Zealand

Abstract

This paper presents a capacitive power transfer (CPT) system using a Class-E resonant inverter. A Class-E resonant inverter is chosen because of its ability to perform DC-to-AC inversion efficiently while significantly reducing switching losses. The proposed CPT system consists of an efficient Class-E resonant inverter and capacitive coupling formed by two flat rectangular transmitter and receiver plates. To understand CPT behavior, we study the effects of various coupling distances on output power performance. The proposed design is verified through lab experiments with a nominal operating frequency of 1 MHz and 0.25 mm coupling gap. An efficiency of 96.3% is achieved. A simple frequency tracking unit is also proposed to tune the operating frequency in response to changes in the coupling gap. With this resonant frequency tracking unit, the efficiency of the proposed CPT system can be maintained within 96.3%–91% for the coupling gap range of 0.25–2 mm.

Key words: Class-E, Capacitive power transfer, Frequency tracking, Wireless power transfer, Zero voltage switching

I. INTRODUCTION

Wireless power transfer (WPT) systems have recently undergone significant development [1] and [2]. WPT is the transmission of electrical energy from a power source to an electrical load without man-made conductors. Innovative technology brings new possibilities of supplying mobile devices with electrical energy without the need for cables, connectors, and/or slip rings. This technology increases the reliability and maintenance-free operation of systems in critical applications, such as aerospace, biomedicine, multisensors, and robotics. Various techniques are categorized according to the medium used for energy transfer; these techniques include acoustics-based WPT, light-based WPT, capacitive-based WPT, and inductive coupled WPT, which is the largest group. Fig. 1 shows the basic block diagram of a WPT system. It consists of a primary side DC-to-AC resonant converter, which converts DC to high frequency AC energy. The AC energy is then transferred via an energy transfer medium to the secondary side receiver. The secondary side is not connected electrically to the primary side and is thus movable (linearly or/and rotating), flexible, mobile, and safe for supplying loads. In the secondary side, high frequency AC energy is converted safely by an AC-to-DC converter to meet the requirements specified by the load parameters. In most cases, a diode rectifier with a capacitive filter is used as an AC-to-DC converter. However, in some applications, an active rectifier or inverter (for stabilizing DC or AC loads) is required.

WPT based on a magnetic field technique has achieved great success in theoretical development and industrial applications for power delivery in certain areas. The magnetic field-based WPT can be adopted in short-range and mid-range applications. The transfer efficiency and transfer power of magnetic induction are normally high, but the transfer distance is limited to a centimeter range with an operating frequency usually within kHz. By contrast, the transfer efficiency and power transfer of magnetic resonance are lower, but the transfer distance can achieve a meter range with an operating frequency roughly in the MHz series

Manuscript received Feb. 1, 2016; accepted May 16, 2016
Recommended for publication by Associate Editor Jee-Hoon Jung.
†Corresponding Author: shakir@utem.edu.my
Tel: +606-5552101, Fax: +606-5552112, Universiti Teknikal Malaysia Melaka
*Advance Sensors & Embedded Control System (ASECS) Research Group, Faculty of Electronics & Computer Engineering, Universiti Teknikal Malaysia Melaka, Malaysia
**Department of Electrical & Computer Engineering, The University of Auckland, New Zealand

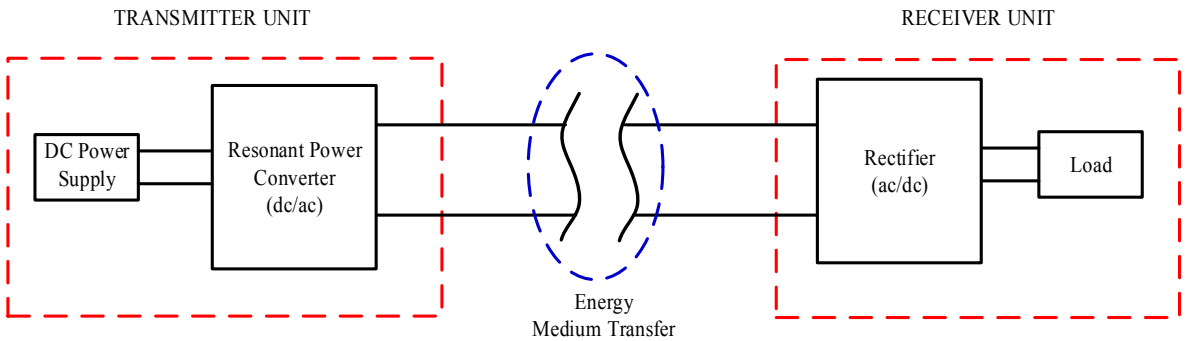

Fig. 1. Block Diagram of WPT System.

[3]-[5]. However, WPT based on a magnetic field has certain limitations: 1) magnetic fields cannot penetrate metals, and thus, magnetic field WPT cannot be used if metal barriers exist between power sources and loads; 2) special shields are needed to prevent electromagnetic interference, and high efficiency magnetic cores are necessary to achieve a reliable coupling factor, which increases the converter size and cost, and potentially reduces mechanical robustness [6]. These limitations can be overcome through capacitive power transfer (CPT) because an electric field can penetrate any metal shielding environment. CPT can transmit through metals and shielded bodies, is cheap to construct, and is flexible in terms of the design of the coupling plate.

With its previous design [1], [6], [7], CPT has rarely been used in high power systems because of its limited power delivery and low efficiency over long distances. Recently, CPT has undergone rapid development from several watt loads to kilowatt-scale loads [8], [9]. Despite such power level advancement, however, the physical limitations in gap distance generally limit the application of CPT, particularly for gap distances greater than 1 mm. In a recent study, Fei Lu et al. [10] proposed a 1.6 kW CPT system with a 300 mm gap distance and 89.1% efficiency. However, large gaps result in kilovolts of potential between the transmitter and receiver plates. Even if the electric field is kept to a safe level for a given frequency, the resulting voltage across the gap may not be safe for human contact. The permitted electric field for human exposure is 600 V/m [11]. This restriction mainly explains the small CPT gaps. At high power and large gaps, the transmitter-to-receiver voltage can become dangerous.

For low wattage applications, CPT systems have exhibited limited output power and efficiency over high gap distances. To improve the efficiency of existing CPT systems over long distances, this study investigates the implementation of a soft-switching topology based on a Class-E resonant inverter. The resonant frequency tracking unit is proposed to achieve the aforementioned objective. The contributions of this paper can be summarized as follows:

1) Design and analysis of an efficient resonant power converter of the transmitter unit in a CPT system. The efficiency of the proposed Class-E resonant inverter is 98.44%. This inverter is powered by 12 Vdc and operated at 1 MHz to produce a stable sinusoidal signal to drive capacitive coupling based on flat rectangular printed circuit board (PCB) plates.
2) For the proposed CPT system with a resonant frequency tracking unit, an output power of 9.03 W is attainable with 2.17 nF of total interface capacitance. The efficiency is 90.3% for a working distance of 2 mm. The effects on output power performance at different capacitive coupling distances are proven through experimental results.

The structure of this paper is organized as follows. Section II explains the CPT concept in detail. Section III reviews the Class-E resonant inverter circuit operation and the equations used to obtain the theoretical value of required components. Section IV discusses circuit design, the implementation of the Class-E resonant inverter circuit, and the experimental results for the basic CPT system and resonant frequency tracking unit. Section V provides the conclusions drawn.

II. Capacitive Power Transfer Concept

The basic structure of the CPT system is shown in Fig. 2. It consists of a transmitter unit, electric field coupler plates, and a receiver unit. The transmitter unit acts as a high-frequency voltage source inverter, which converts standard frequency DC power supply to high frequency AC voltage. Several types of inverter can be used on the transmitting side; these types include push–pull resonant inverters [12], Class-D inverters, Class-E inverters [13], Class-F inverters, and other resonant converter topologies [14].

Electric field coupling plates serve the energy transfer medium for CPT systems. The electric field coupler functions as two capacitors connected in series during CPT operation. CPT system operation requires a high frequency voltage to drive the two primary metal plates. When two secondary plates are placed in close proximity to the primary metal plates, an alternating electric field is formed between the plates, causing a displacement current that flows through it. Consequently, power can be transferred to the load without direct electrical contact while allowing some freedom of

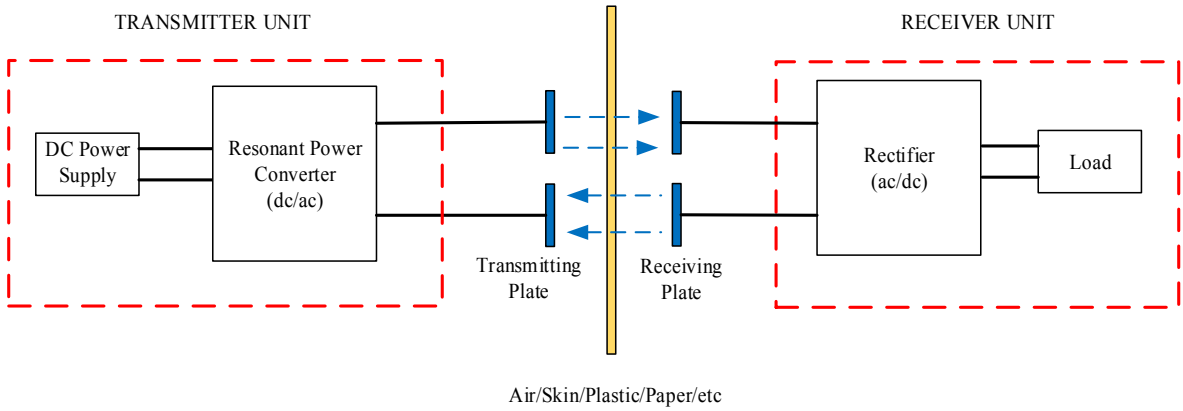

Fig. 2. Block Diagram of Typical CPT System.

movement between the primary and secondary plates. The capacitive coupling structure can be of various configurations according to different applications; it may be rectangular, cylinder, disk [15], matrix [16], conformal surface [17], and hydrodynamic capacitive coupling [18], [19].

The receiver unit regulates the captured power and drives the load according to demand. In most cases, the power captured by the receiver side cannot be used directly by the load. The rectifier circuit in the receiver unit usually comes with the power flow controls to regulate captured power (Fig. 2). In the case of powering moveable load, any position change at the receiver side can result in a mismatch between the coupling plates. This mismatch can cause a significant voltage drop and degrade the power transfer capacity. Power flow control circuits are often necessary to maintain the output power at a constant level.

The power converter converts power and acts as a control circuit. According to previous works, the half-bridge inverter is suitable for CPT systems because of its simplicity and attainment of zero voltage switching (ZVS) without additional control circuits [20], [21]. Unlike single switch converters, full and half-bridge inverters and push–pull converters are composed of several semiconductors and gate drivers and exhibit a complicated board layout. Other types of high frequency resonant inverters must be investigated further. Generally, high frequency inverters, such as Class-D or Class-E inverters, are the most suitable candidates for WPT systems because of their high efficiency that approaches 100% theoretical efficiency [17], [22], [23]. Jiejian Dai et al. proposed four types of single active switch power electronics (i.e., Cuk, SEPIC, Zeta, and buck-boost) for a kW scale CPT system with over 90% efficiency [9]. The present work proposes a high efficiency Class-E resonant inverter for low wattage CPT applications. Unlike other types of high frequency inverters, the Class-E inverter comprises fewer components and is thus highly reliable.

III. Review of Class-E Resonant Inverter Concept

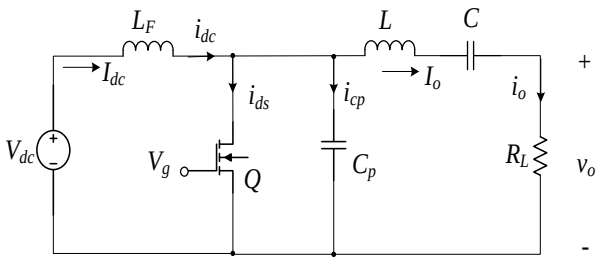

Fig. 3. Typical Class-E Circuit.

An analysis of the Class-E resonant inverter (Fig. 3) is carried out under the following assumptions:

1) The MOSFET and diode form an ideal switch in which on-resistance is zero, off-resistance is infinity, and switching times are zero.
2) The choke inductance is high enough that the AC component is much lower than the DC component of the input current.
3) The loaded quality factor Q of the L, C, and R_L series-resonant circuit is high enough so that current I through the resonant circuit is sinusoidal.
4) All circuit elements are ideal.
5) The duty cycle is 50%.

With regard to Fig. 3 and the given assumptions, output current i_o can be defined as

$$i_o = I_m \sin(\omega t + \varphi) \tag{1}$$

where I_m is the output current amplitude and φ is the initial phase of the current i_o. Furthermore,

$$i_{ds} + i_{Cp} = I_{dc} - i_o = I_{dc} - I_m \sin(\omega t + \varphi) \tag{2}$$

The switch is on for the time interval $0 < \omega t \leq \pi$. Therefore, $i_{cp} = 0$. The current through the switch is given by

$$i_{ds} = \begin{cases} I_{dc} - I_m \sin(\omega t + \varphi), & for\ 0 < \omega t \leq DT \\ 0, & for\ DT < \omega t \leq T \end{cases} \tag{3}$$

The switch is off for the time interval $\pi < \omega t < 2\pi$, which implies that $i_{ds} = 0$. Consequently, the current through the shunt capacitance is

$$i_{Cp} = \begin{cases} 0, & for\ 0 < \omega t \leq DT \\ I_{dc} - I_m \sin(\omega t + \varphi), & for\ DT < \omega t \leq T \end{cases} \tag{4}$$

Using (4), the switch voltage, v_{ds} is given as

$$v_{ds} = \frac{1}{\omega Cp}\int_{DT}^{\omega t} i_{Cp}\, d(\omega t) = \begin{cases} 0, & for\ 0 < \omega t \le DT \\ \frac{1}{\omega Cp}\left\{ I_{dc}(\omega t - DT) + I_m \cos(\omega t + \varphi) \right\}, & for\ DT < \omega t \le T \\ -\cos(DT + \varphi) \end{cases} \quad (5)$$

Substituting the condition v_{ds} (2π) = 0 into (5) yields the following relationship among I_{dc}, I_m, D, and φ:

$$I_m = I_{dc}\frac{T(1-D)}{\cos(DT+\varphi)-cos\varphi} \quad (6)$$

Furthermore, using (2) at ωt = 2π, (5), and (6), the relationship between φ and duty cycle D can be written as

$$tan\,\varphi = \frac{cosDT-1}{T(1-D)+sinDT} \quad (7)$$

Thus,

$$\varphi = \pi + arctan\left[\frac{cosDT-1}{T(1-D)+sinDT}\right] \quad (8)$$

The parameters of the circuit shown in Fig. 3 at optimum operation are as follows:

The full load resistance is

$$R_L = \frac{8V_{CC}^2}{(\pi^2+4)P} \quad (9)$$

where P is the output power. The component values for the load network are

$$C_p = \frac{I_o}{\omega\pi V_{CC}^2} = \frac{1}{\omega\pi\left(\frac{\pi^2}{4}+1\right)\frac{\pi}{2}} \quad (10)$$

$$C = \frac{1}{\omega R\left(Q-\frac{\pi(\pi^2-4)}{16}\right)} \quad (11)$$

$$L = \frac{QR_L}{\omega} \quad (12)$$

and the choke inductor is

$$L_{f(min)} = 2\left(\frac{\pi^2}{4}+1\right)\frac{R}{f} \quad (13)$$

The assumptions and derivations of the circuit are similar to those presented in [24].

IV. Circuit Design and Implementation

The proposed CPT system consists of a Class-E resonant inverter and capacitive coupling. Both parts should be carefully designed. The performance of the Class-E resonant inverter with respect to operating frequency, load, and duty cycle were analyzed. The generation of the Class-E resonant inverter in the transmitter unit is important to the performance of the whole system as it affects energy transfer efficiency. The effect of varying capacitive coupling distances on output power performance was studied. The proposed system was designed and simulated with Proteus 8 Professional software. The proposed concept was validated by conducting a laboratory experiment for the CPT system. The experimental setup for the complete CPT system was implemented with discrete components on a PCB. The components were chosen to match the design as closely as possible. The voltage and current of the designed system were measured to analyze performance in terms of input power, output power, and efficiency. For input power $P_{i(dc)}$, DC voltage and current data were collected with a Sanwa CD771 Digital Multimeter. For output $P_{o(ac)}$, an Agilent Technologies DSO-X 2012A 100 MHz oscilloscope was used to obtain the voltage waveforms. Efficiency percentage was measured by finding the ratio of input power to output power. The following section discusses the results.

A. Analysis of Class-E Resonant Inverter

To validate the simulation results, we conducted the experiment at an operating frequency of 1 MHz, which was sufficiently large to minimize the coupling capacitor impedance and thereby achieve a small coupling plate size. Power MOSFET IRF510 was chosen because of its capability as a switching device of resonant inverters at high frequencies. According to IRF510 MOSFET datasheets, it is an n-channel enhancement mode and is designed especially for high speed applications. The breakdown switch voltage and current were 100 V and 5.5 A, respectively. According to (5), the peak switch voltage and current were 42.74 V and 2.39 A, respectively, which confirm the suitability of the IRF510 MOSFET for the Class-E resonant inverter.

The SK40C microcontroller board with PIC16F887A was used to generate the desired switching control signal frequency at 50% duty cycle for the MOSFET gate. However, the microcontroller output voltage, which is typically 5 V, was not sufficient to turn on the IRF510 MOSFET, which requires at least 10 V to operate safely. An IC gate drive TC4422 was used to provide sufficient gate voltage/charge to drive the IRF510 MOSFET. The complete experimental setup is shown in Fig. 4.

Fig. 5 shows the waveforms obtained from the Proteus simulation and circuit experiment of the Class-E resonant inverter circuit. Fig. 5(a) shows that the simulated maximum voltage across the MOSFET during the turn-off state was $V_{ds(peak)}$ = 41 V, which is nearly three times larger than Vcc. During the turn-on state, $V_{ds(peak)}$ = 4.5 V, which is nearly 11% of the peak switch voltage. In an optimum design yielding maximum drain efficiency, the switch voltage V_{ds} at the turn-on state is 10% to 50% of the peak switch voltage under nonzero voltage switching conditions. In Fig. 5(b), the experimental maximum voltage across the MOSFET during the turn-off state was $V_{ds(peak)}$ = 37.8 V, which is 8.75% lower than the simulated value. During the turn-on state, $V_{ds(peak)}$ = 4 V, which is nearly 10% of the switch peak voltage. The experiment value of the peak output voltage $V_{RL(peak)}$ was 12.35 V, which is 2.9 % higher than the simulated value.

The results of the simulation and experiment were consistent with the theoretical predictions. This good agreement indicates that the optimum operation can be achieved only at optimum load resistance, $R_L = R_{opt}$. When $R_L = R_{opt}$, the sinusoidal output voltage nearly reaches the

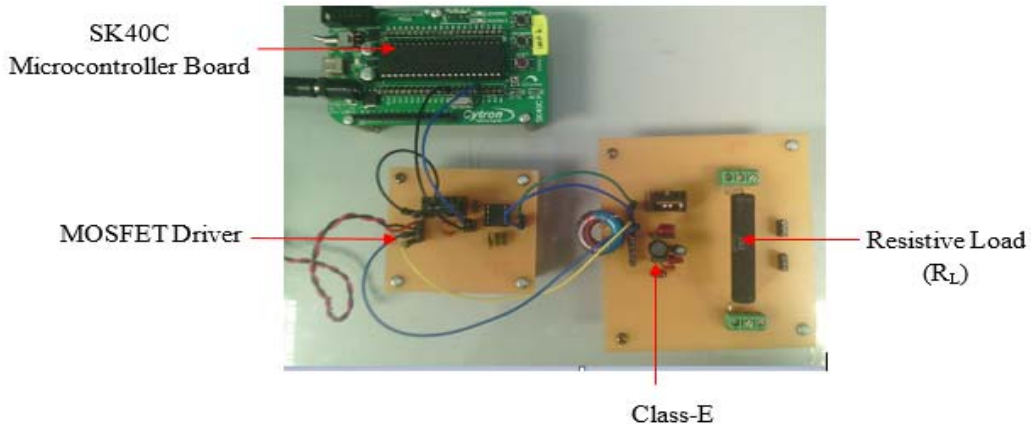

Fig. 4. Experimental Setup for Class-E Resonant Inverter.

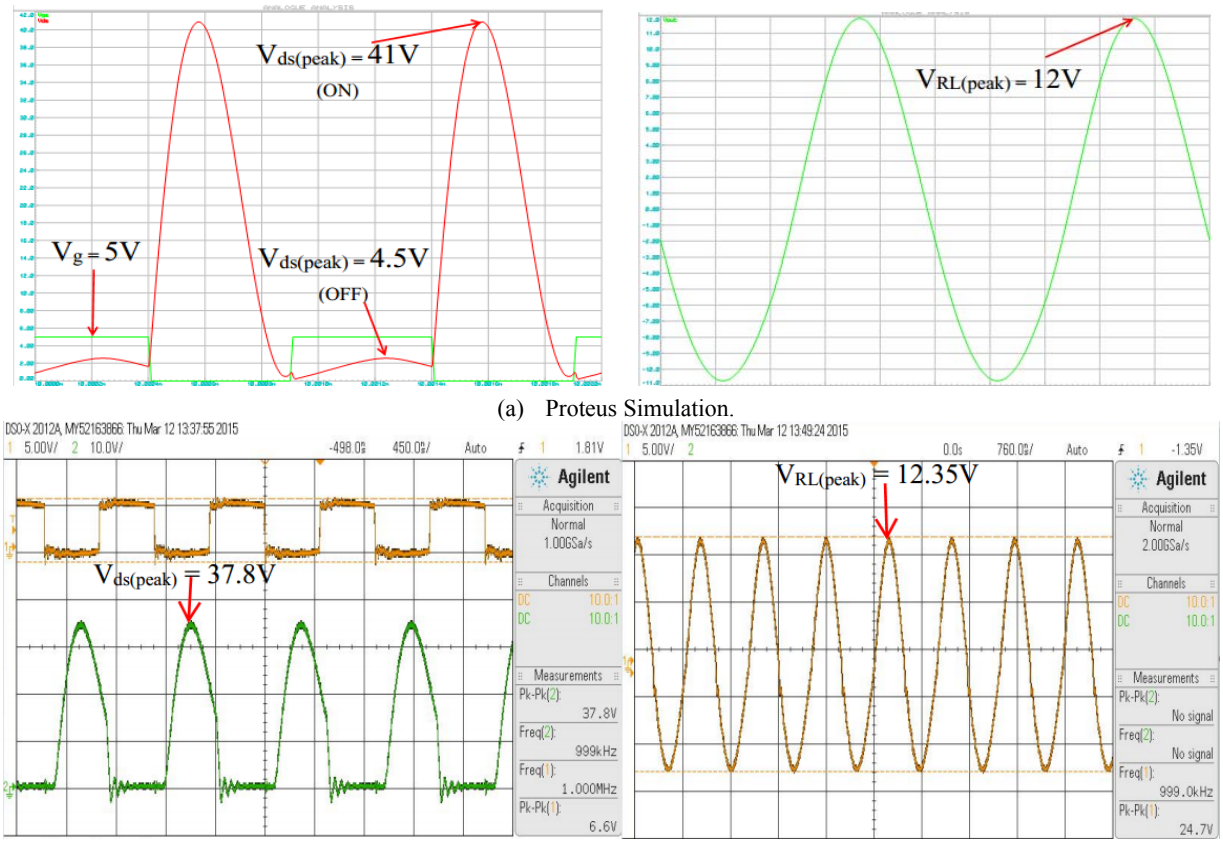

(a) Proteus Simulation.

(b) Circuit Experiment.

Fig. 5. Input, Switching Voltage and Output Voltage Waveforms for the First Design at 1 MHz Frequency.

maximum. Furthermore, the experimental switching voltage waveform proves that the Class-E resonant inverter circuit using PIC16F877A satisfies ZVS conditions because of the absence of an overlap between the voltage over the MOSFET channel and the current through the channel. The efficiency of the experimental circuit was 98.4%, which is 11.05% higher than the simulated value. This result is attributed to the use of non-pure resistive load, which resulted in the artificially high efficiency of the experimental work.

B. Analysis of Capacitive Power Transfer

This section focuses on modifying the proposed Class-E resonant inverter to fit a CPT system. Fig. 6 shows the proposed CPT block diagram. It consists of a Class-E resonant inverter and PIC microcontroller circuit, which generates a desired switching control signal frequency at 50% duty cycle for the MOSFET gate. Both components serve as a transmitter unit. As the Class-E resonant inverter in Fig. 3 has a series capacitor at the load network output, one of the

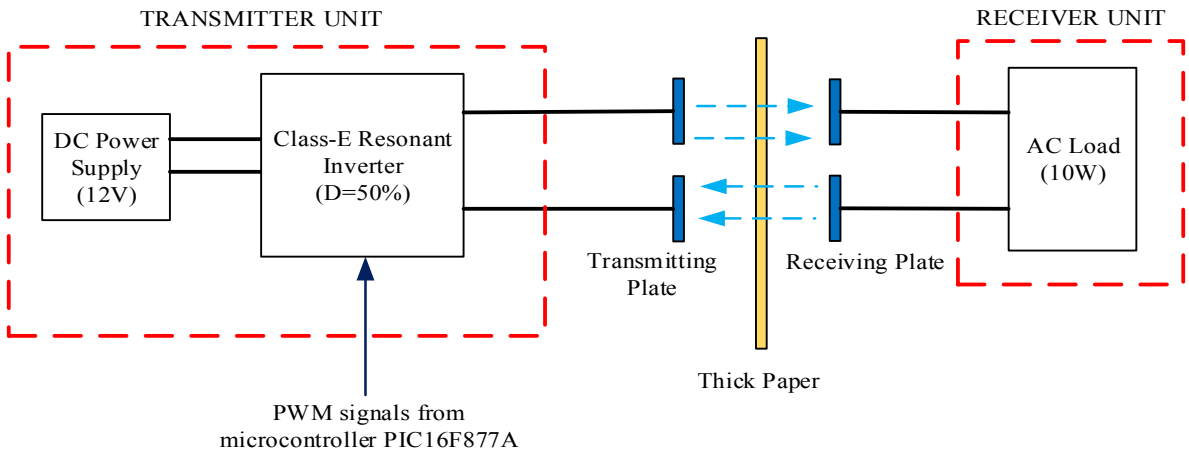

Fig. 6. Proposed CPT System Block Diagram.

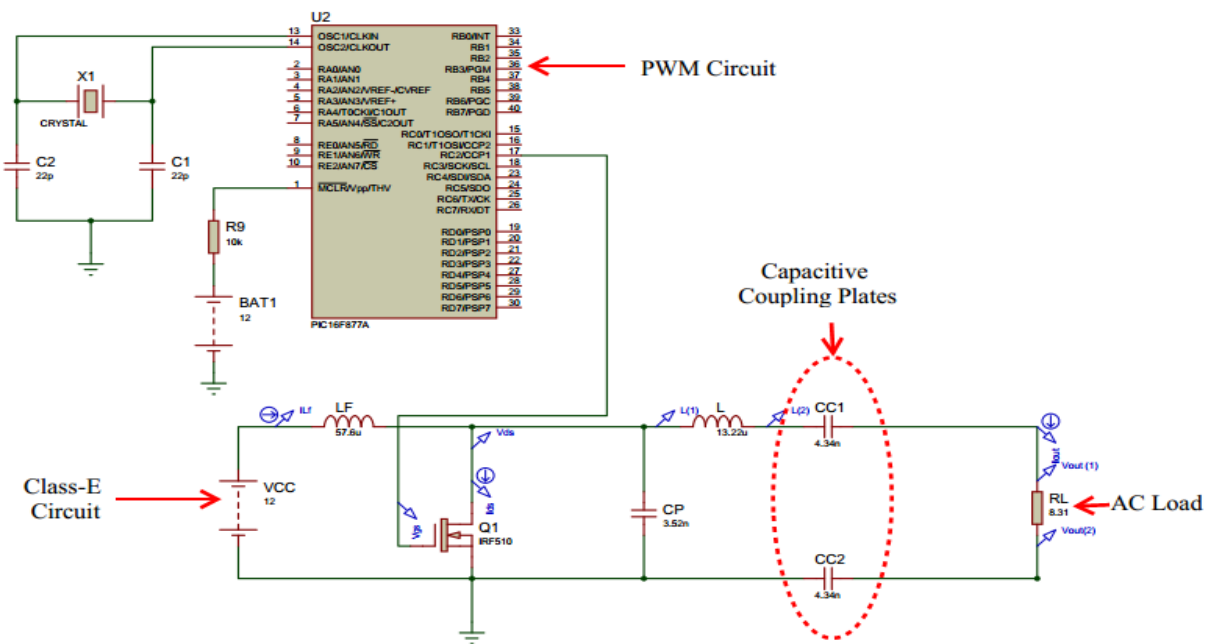

Fig. 7. Proposed CPT System Model in Proteus Software.

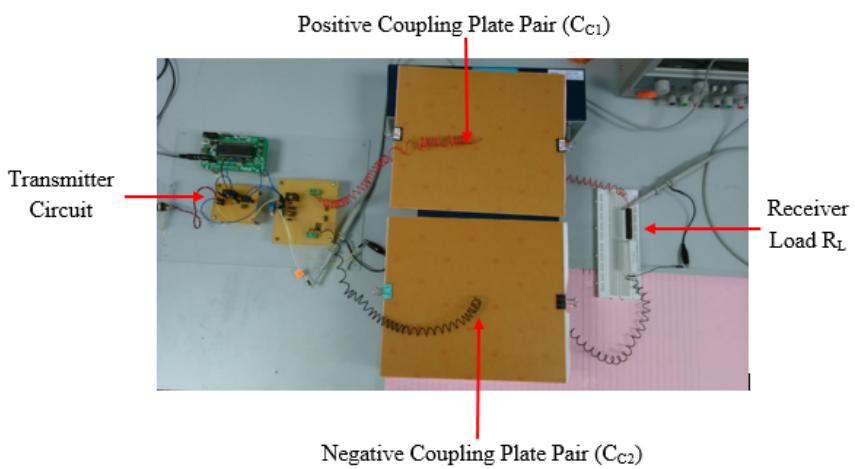

Fig. 8. Proposed CPT System Experimental Setup.

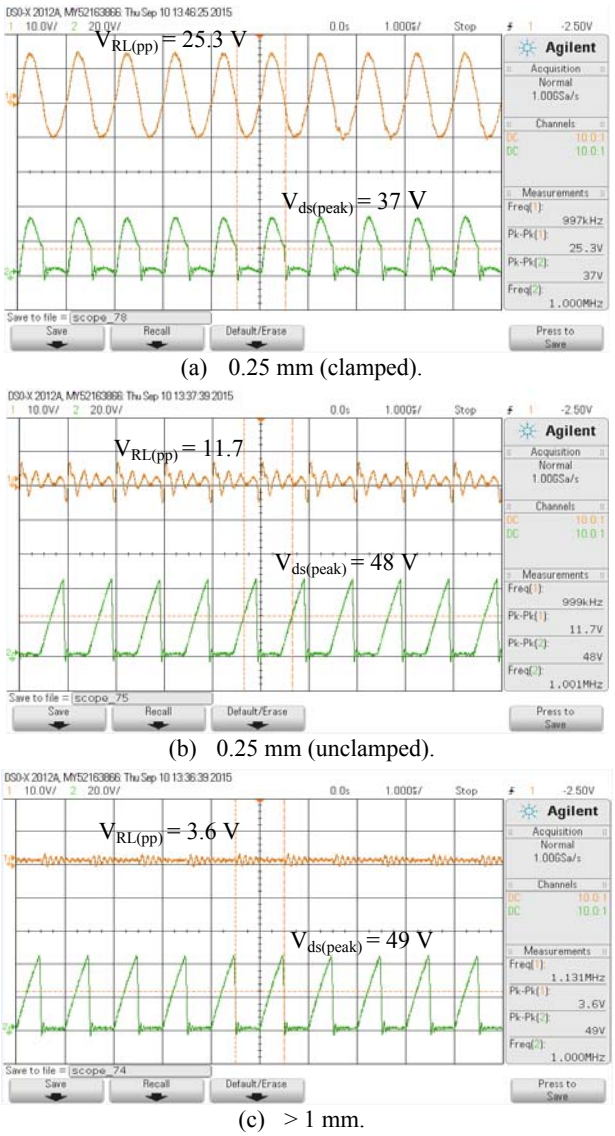

Fig. 9. Experimental Waveforms of Receiver Plate Voltage, V_{RL}, and Switch Voltage, V_{DS}, at Different Coupling Plate Distances.

capacitors can be modified to fit the CPT system easily. Figs. 7 and 8 show that four coupling plates were used to form two pairs of capacitors, C_{C1} and C_{C2}, in the series resonant tank. As the result of the modification, the total capacitance of the coupling plates, which is denoted as C and illustrated in Fig. 3, became equal to $C_{C1}\cdot C_{C2}/(C_{C1}+C_{C2})$ and formed a series resonant tank. R_L is the AC load, which can also be treated as the input resistance of a rectifier if a DC load is required. In practice, most WPT loads are DC. A required DC load may be obtained by simply adding a matching load [25] and high frequency rectifier circuit, such as a Class-E rectifier at the receiver unit.

The capacitive coupling interface was implemented with rectangular PCB plate capacitors separated by a piece of thick paper. The initial gap was assumed to be 0.25 mm (thickness of the paper) with a dielectric constant of 2.5. The plate size was therefore 0.04904 m^2, with a combined interface

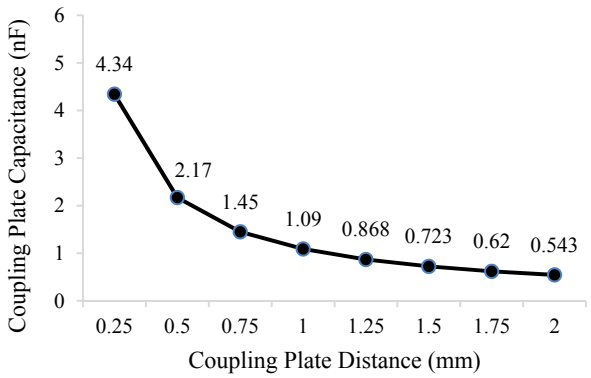

Fig.10. Capacitance vs. Distance.

capacitance of 2.17 nF. The PCB plates were clamped together to minimize capacitance variations caused by imperfect flatness, which would otherwise cause an uneven distribution of the air gap and low coupling capacitance. The effects of varying plate distances on output power performance were investigated, and the working distance was limited to 0.25–2 mm.

An experimental setup for a complete CPT system with a rectangular coupling structure was used to validate the proposed concept. As shown in Fig. 9(a), the experimental peak voltage indicated at the receiver plate, which is the voltage across R_L (V_{RL}) is 12.65 V. They were measured with the plates C_{C1} and C_{C2} clamped together, with an initial gap distance of 0.25 mm. The experimental value of the AC output power, $P_{o(ac)}$, was calculated using $P_{o(ac)} = (V_{RL(rms)})^2/R_L$ = 9.63 W, which indicated that the proposed systems could transfer 9.63 W to the load with 96.3% efficiency.

As shown in Fig. 9(b), the peak receiver plate voltage was 5.75 V, which was measured when the gap distance was 025 mm and without clamping the coupling plates. At an initial gap distance greater than 1 mm (Fig. 9(c)), the peak receiver plate voltage decreased drastically to 1.8 V and moved toward 0 V as the gap distance increased to 2 mm. Furthermore, the output voltage waveforms transferred to the load were not purely sinusoidal waves because of the imperfect flatness, which caused impedance matching problems. The results show that this behavior can be correlated with the equivalent capacitance equation of each of the coupling plates. This equation is expressed as

$$C = \frac{A\varepsilon_0\varepsilon_r}{d} \tag{14}$$

where A, d, ε_0, and ε_r denote the effective coupling area, coupling distance, permittivity in vacuum, and relative permittivity of the dielectric material between the coupling plates, respectively. Equation (14) shows that the capacitance is directly proportional to the dielectric constant and physical size of the plates, as determined by the plate area. Capacitance is inversely proportional to the distance between the plates (Fig. 10).

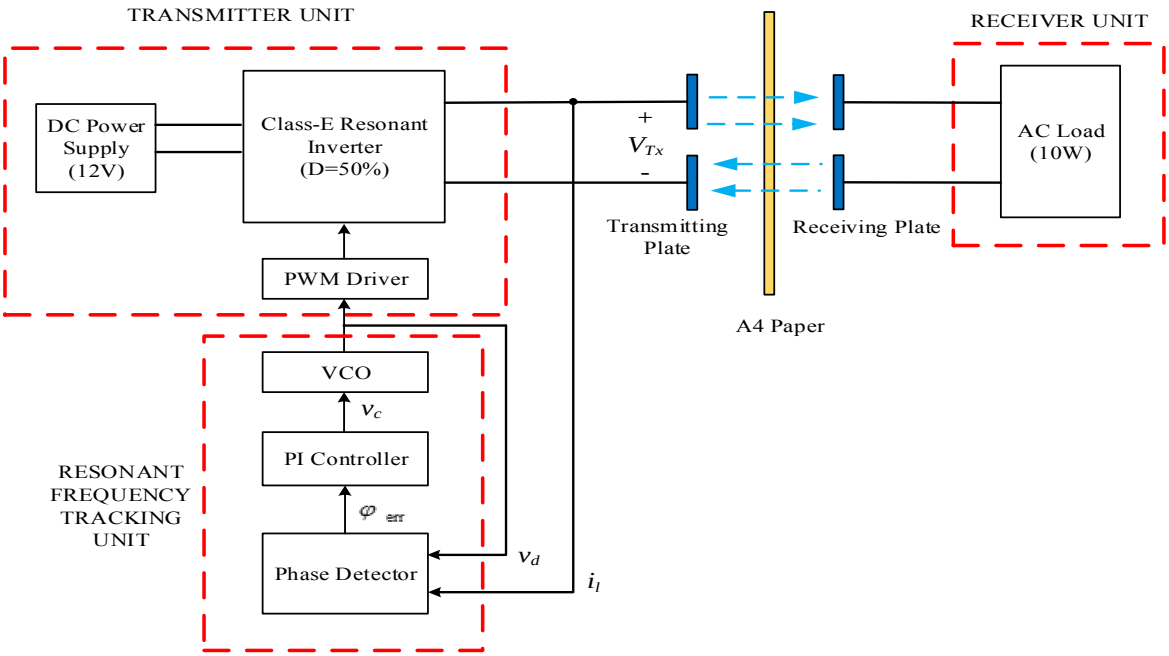

Fig. 11. Proposed CPT System with FTU Block Diagram.

C. Capacitive Power Transfer System with Frequency Tracking Unit (FTU)

This section presents the experimental results to validate the proposed CPT system with a resonant frequency tracking unit (Fig. 11). According to the analysis in the previous section, the CPT system is sensitive to the amount of coupling plate capacitance; hence, the coupling plates must be clamped to maintain maximum efficiency. The efficiency of the system can only reach 96.3% if the gap distance is 0.25 mm. It then drops abruptly if the distance is increased because of the variation of impedance matching while adjusting the coupling plate distances (see Fig. 10). To overcome the problems, we proposed a CPT system with a resonant frequency tracking unit capable of tuning the Class-E inverter switching frequency. The coupling distance between plates CC1/CC2 is normally unknown in real applications because of the placement of secondary plates in the receiver unit. To make the power transfer efficiency insensitive to the exact coupling capacitance, the feedback frequency tracking unit tunes the frequency such that it is near the resonant frequency of the system, $f = 1/2\pi\sqrt{LC}$.

The resonant frequency tracking unit consists of a phase detector, proportional integral (PI) controller, and voltage control oscillator (VCO) (Fig. 11). The sampled waveforms i_l and v_d are sent to the phase detector, which generates a pulse voltage representing the phase difference (φ_{pd}) between the inputs. Let the deviation angle $\varphi_{err} = \varphi_{ref} - \varphi_{pd}$. The ultimate goal of the design is to obtain $\varphi_{err} = 0$. The deviation error is then adjusted with the PI controller to produce a control voltage v_c, which is used to set the phase of the VCO. When the system is functioning properly, the loop adjusts the control voltage v_c, which drives the phase deviation to zero. Theoretically, the optimum phase (φ_{ref}) for the Class-E resonant inverter is −32.48° [19]. The resonant frequency tracking unit must be able to track the phase difference of the current i_l and voltage v_d and maintain the phase at −32.48° to yield ZVS operation.

Fig. 12 shows the switching voltage waveforms for CPT systems with and without a frequency tracking unit for distances of 1 and 2 mm, respectively. The proposed PI controller manages to automatically tune the switching frequency to ensure ZVS despite changes in the coupling gap distance. Moreover, the resonant frequency of the system improves when the distance between the transmitter plate and the receiver plate increases. The resonant frequency tracking unit attempts to tune the switching frequency following the change in resonant frequency, as shown in Table I. Comparing the performances of the CPT system with and without a frequency tracking unit in Fig. 13, we find that the efficiency of the system with the tracking unit is successfully maintained at over 90% and operated safely for working distances of up to 2 mm. For gaps of over 2 mm, the frequency increases until the voltage in the transmitter unit V_{Tx} reaches its maximum limit. This limitation is determined by the maximum permissible drain-to-source voltage of IRF510 MOSFET. Currently, the highest gap in low watt scale research for CPT systems is 0.8 mm with 94.3% efficiency [26]. The most obvious finding to emerge from this study is that a high efficiency at higher coupling gap distances can be obtained using the aforementioned technique.

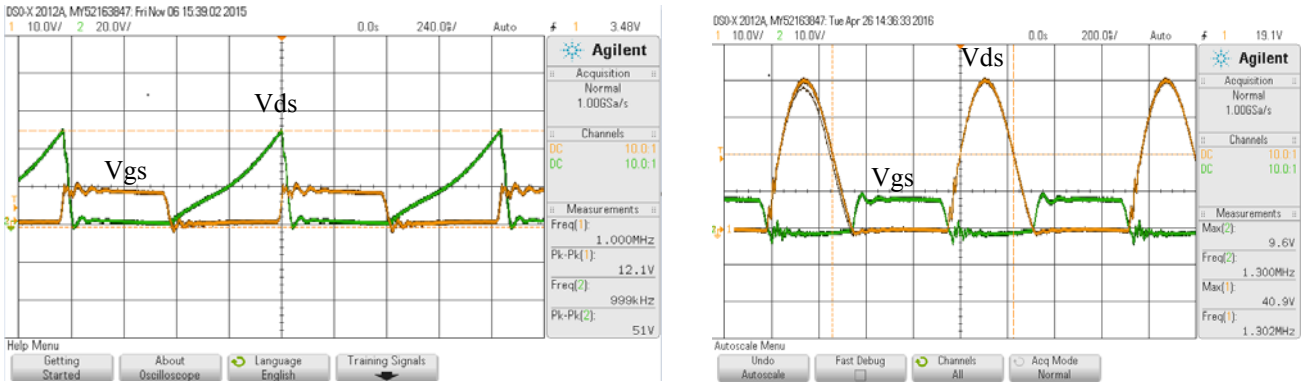

i - without FTU ii - with FTU

(a) d = 1 mm.

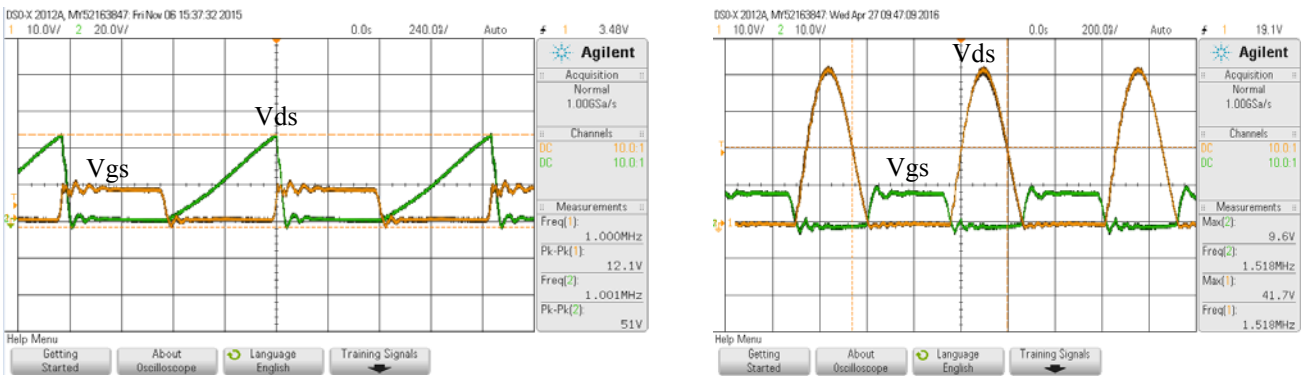

i - without FTU ii - with FTU

(b) d = 2 mm.

Fig. 12. Experimental Waveforms of Switching Voltage at Different Coupling Gap Distances.

TABLE I
CPT SYSTEM WITH FTU OUTPUT PARAMETER

Parameter		Plate Distance (mm)							
		0.25	**0.5**	**0.75**	**1**	**1.25**	**1.5**	**1.75**	**2**
V_{RL} (peak)	V	12.85	12.8	12.7	12.65	12.4	12.3	12.25	12.25
f	MHz	1.08	1.15	1.23	1.32	1.4	1.48	1.5	1.51
Po	W	9.94	9.86	9.7	9.64	9.25	9.1	9.03	9.03
η	%	99.4	98.6	97	96.4	92.5	91	90.3	90.3

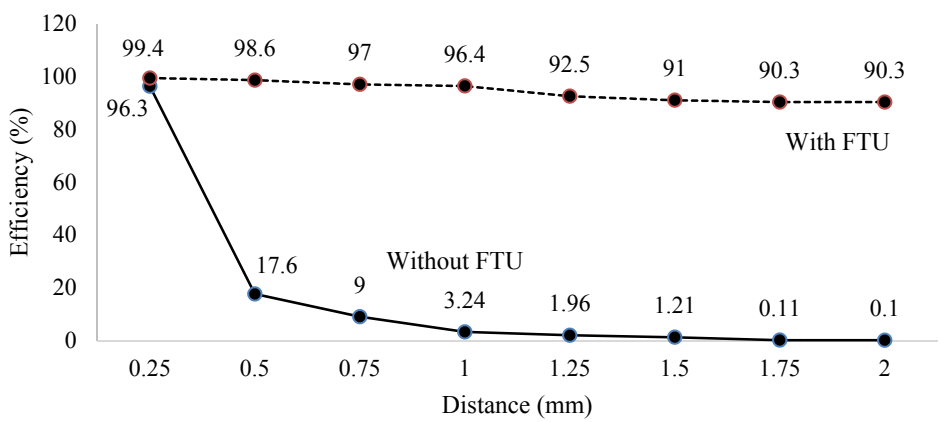

Fig. 13. Efficiency vs. Coupling Gap Distance with and without FTU.

V. CONCLUSION

An analysis of CPT systems using a Class-E resonant inverter is presented. The power converter requirement for the system on the transmitter side is analyzed through an experiment. The efficiency of the Class-E resonant inverter is 98.44% when powered by 12 Vdc and operated at a frequency of 1 MHz to produce a stable sinusoidal signal and thereby drive the capacitive coupling based on flat rectangular copper plates. The system is unable to maintain such efficiency at a high level when the coupling gap distance is increased. Therefore, the existing CPT system is improved by adding a resonant frequency tracking controller to help the CPT system in maximizing the power transfer efficiency by allowing variations in the coupling gap distance. For the second part of the experiment, the output power efficiency of different coupling gap distances of up to 2 mm is analyzed. The proposed CPT system with resonant frequency tracking generates 9.03 W output power through a combined interface (PCB plate) capacitance of 2.17 nF at 2 mm working distance and achieves a 90.3% efficiency. The agreement between the experimental performance and theoretical performance can be considered excellent. For its future development, this system will be applied in rotary applications, such as fluid bearing capacitors and rotating capacitors. Hydrodynamic capacitive coupling is also attractive for such applications [19], as they can provide high coupling capacitance for high power rotary applications, such as slip ring replacement. However, they may have speed-dependent coupling capacitance, and the circuit must be auto-tuned. Additionally, conformal pads have been developed for CPT [17]. The pads shape and mold themselves to surfaces for maximum coupling. The capacitance may change when force is applied. In both of these situations, the proposed CPT system with a frequency tracking unit for Class-E inverters would be applicable.

ACKNOWLEDGMENT

This research was supported by the Universiti Teknikal Malaysia Melaka (UTeM) [RAGS/1/2014/TK03/FKEKK/B00062] and Malaysian Ministry of Education [FRGS/2/2014/TK03/FKEKK/03/F00243] grants.

REFERENCES

[1] M. Kline, I. Izyumin, B. Boser, and S. Sanders, "Capacitive power transfer for contactless charging," *Twenty-Sixth Annual IEEE Applied Power Electronics Conference and Exposition (APEC)*, pp. 1398-1404, 2011.

[2] T. Duong and J.W. Lee, "A dynamically adaptable impedance-matching system for midrange wireless power transfer with misalignment," *Energies*, Vol. 8, No. 8, pp. 7593-7617, Jul. 2015.

[3] J. Huh, W. Lee, S. Choi, G. Cho, and C. Rim, "Frequency domain circuit model and analysis of coupled magnetic resonance systems," *Journal of Power Electronics*, Vol. 13, No. 2, pp. 275-286, Mar. 2013.

[4] X. Wei, Z. Wang, and H. Dai, "A critical review of wireless power transfer via strongly coupled magnetic resonances," *Energies*, Vol. 7, No. 7, pp. 4316-4341, Jul. 2014.

[5] A. Kurs, A. Karalis, R. Moffatt, J. D. Joannopoulos, P. Fisher, M. Soljacic, and M. Soljac, "Wireless power transfer via strongly coupled magnetic resonances," *Science*, Vol. 317, pp. 83-86, Jul. 2007.

[6] M. P. Theodoridis, "Effective capacitive power transfer," *IEEE Trans. Power Electron.*, Vol. 27, No. 12, pp. 4906-4913, Dec. 2012.

[7] C. Liu and A. P. Hu "Steady state analysis of a capacitively coupled contactless power transfer system," *IEEE Energy Convers. Congr. Expo.*, pp. 3233-3238, 2009.

[8] J. Dai and D. Ludois, "A survey of wireless power transfer and a critical comparison of inductive and capacitive coupling for small gap applications," *IEEE Trans. Power Electron.*, Vol. 30, No. 11, pp. 6017-6029, Nov. 2015.

[9] J. Dai and D. C. Ludois, "Single active switch power electronics for kilowatt scale capacitive power transfer," *IEEE J. Emerg. Sel. Top. Power Electron.*, Vol. 3, No. 1, pp. 315-323, Mar. 2015.

[10] Feu Lu, Hua Zhang, Heath Hofmann, and C. Mi, "A double-sided LCLC-compensated capacitive power transfer system for electric vehicle charging," *IEEE Trans. Power Electron.*, Vol. 30, No. 11, pp. 6011-6014, Nov. 2015.

[11] *IEEE Standards Coordinating Committee 28*, *IEEE C95. 1-1992: IEEE Standard for Safety Levels with Respect to Human Exposure to Radio Frequency Electromagnetic Fields, 3 kHz to 300 GHz*, 2006.

[12] C. Liu, A. P. Hu, and N.-K. C. Nair, "Modelling and analysis of a capacitively coupled contactless power transfer system," *IET Power Electron.*, Vol. 4, No. 7, pp. 808-815, Aug. 2011.

[13] Y. Yusmarnita, S. Saat, A. H. Hamidon, H. Husin, N. Jamal, K. Kh, and I. Hindustan, "Design and analysis of 1MHz class-E power amplifier," *WSEAS Trans. Circuits and Systems*, Vol. 7, Jun. 2016.

[14] M. Hannan, H. Hussein, S. Mutashar, S. Samad, and A. Hussain, "Automatic frequency controller for power amplifiers used in bio-implanted applications: Issues and challenges," *Sensors*, Vol. 14, No. 12, pp. 23843-23870, Dec. 2014.

[15] C. Liu, A. P. Hu, and N.-K. C. Nair, "Coupling study of a rotary capacitive power transfer system," *IEEE International Conference on Industrial Technology*, pp. 1-6, 2009.

[16] C. Liu, A. P. Hu, and X. Dai, "A contactless power transfer system with capacitively coupled matrix pad," in *2011 IEEE Energy Conversion Congress and Exposition*, pp. 3488-3494, 2011.

[17] J. Dai, S. Member, D. C. Ludois, and M. Ieee, "Wireless electric vehicle charging via capacitive power transfer through a conformal bumper," *IEEE Applied Power Electronics Conference and Exposition (APEC)*, pp. 3307-3313, 2015.

[18] D. C. Ludois, M. J. Erickson, and J. K. Reed, "Aerodynamic fluid bearings for translational and rotating capacitors in noncontact capacitive power transfer systems," *IEEE Trans. Ind. Appl.*, Vol. 50, No. 2, pp. 1025-1033, Apr. 2014.

[19] S. Hagen, R. Knippel, J. Dai, and D. C. Ludois, "Capacitive coupling through a hydrodynamic journal

bearing to power rotating electrical loads without contact," *IEEE Wireless Power Transfer Conference (WPTC)*, pp. 1-4, 2015.
[20] F. Hirohito and Y. Chiku, "A novel power converter suitable for contactless power distribution with capacitive coupling using series-connected switched-mode active negative capacitor," *Proc. 2011 14th Eur. Conf. Power Electron. Appl.*, pp. 1-8, 2011.
[21] K. H. Yi, "6.78MHz capacitive coupling wireless power transfer system," *Journal of Power Electronics*, Vol. 15, No. 4, pp. 987-993, Jul. 2015.
[22] H.-S. Chong, D.-Y. Lee, and D.-S. Hyun, "A new control scheme of class-E electronic ballast with low crest factor," *Journal of Power Electronics*,Vol. 3, No. 3, pp. 169-188, Jul. 2003.
[23] N. Jamal, S. Saat, and Y. Yusmarnita, "A study on performance of class E converter circuit for loosely coupled inductive power transfer," *WSEAS Trans. Circuits Syst.*,Vol. 13, No. 1, pp. 1-4, Jun. 2014.
[24] M. K. Kazimierczuk and D. Czarkowski, *Resonant Power Converters*, Chapter 12, pp. 334-368, 2011.
[25] K. Lu and S. K. Nguang, "Design of auto-tuning capacitive power transfer system for wireless power transfer," *Int. J. Electron.*, DOI:10.1080/00207217.2015. 1122097, Dec. 2015.
[26] D. C. Ludois, K. Hanson, and J. K. Reed, "Capacitive power transfer for slip ring replacement in wound field synchronous machines," *IEEE Energy Conversion Congress and Exposition*, pp. 1664-1669, 2011.

Yusmarnita Yusop was born in Melaka, Malaysia, in 1979. She received her B. Eng. Degree in Electrical Engineering (Mechatronic) from the University of Technology, Malaysia, in 2001, and her M. Eng. Degree in Electrical Engineering from Tun Hussein Onn University of Malaysia, in 2004. She was appointed Engineering Instructor (2002) at Kolej Universiti Teknikal Malaysia Melaka and promoted to Lecturer (2005) and Senior Lecturer (2008) in the Department of Industrial Electronics, Faculty of Electronic and Computer Engineering at Universiti Teknikal Malaysia Melaka. She has taught many subjects, such as Power Electronics, Advanced Power Electronics, Electronic Systems, and Manufacturing Automation. She is currently working toward her Ph.D. degree. Her research interests include electronic system design, power electronics converters, and wireless power transfer.

Shakir Saat was born in Kedah, Malaysia, in 1981. He received his B. Eng. and M. Eng. degrees in Electrical Engineering from the Universiti Teknologi Malaysia, Malaysia, in 2002 and 2006, respectively, and his Ph.D. degree in Electrical Engineering (Nonlinear Control Theory) from the University of Auckland, New Zealand, in 2013. He is a Senior Lecturer and Deputy Dean (Academic) at the Faculty of Electronic and Computer Engineering, Universiti Teknikal Malaysia Melaka. He has published many articles in high quality journals. His research interests include nonlinear control theory, polynomial discrete-time systems, networked control systems, and wireless power transfer technologies.

Sing Kiong Nguang received his B.E. (with first class honors) and Ph.D. degrees from the Department of Electrical and Computer Engineering of the University of Newcastle, Australia, in 1992 and 1995, respectively. He is a Professor at the Department of Electrical & Computer Engineering at the University of Auckland. He has published 6 books and over 300 refereed journal and conference papers on nonlinear control design, nonlinear control systems, nonlinear time-delay systems, nonlinear sampled-data systems, biomedical systems modeling, fuzzy modeling and control, biological systems modeling and control, and food and bio product processing. He has served on the editorial board of a number of international journals. He is the Chief Editor of the International Journal of Sensors, Wireless Communications and Control.

Huzaimah Husin received her B.Eng. degree (2000) from Multimedia University and her M. Eng. Degree (2005) from Kolej Universiti Tun Hussein Onn, Malaysia. She was appointed Engineering Instructor (2001) at Kolej Universiti Teknikal Malaysia Melaka and promoted to Lecturer (2005) and Senior Lecturer (2008) in the Department of Industrial Electronics, Faculty of Electronic and Computer Engineering at Universiti Teknikal Malaysia Melaka. Since September 2014, she has been pursuing her Ph.D. degree in Advanced Control Technology with a focus on acoustics energy transfer.

Zamre Ghani received his B.Sc. degree in Electrical Engineering from the University of the Pacific, Stockton, California, USA; his M.Eng. degree in Electrical Engineering from Universiti Teknologi Malaysia (UTM); and his Ph.D. degree in Electrical, Electronic & Systems Engineering from Universiti Kebangsaan Malaysia (UKM) in 1987, 2007, and 2014, respectively. He is a Senior Lecturer at the Department of Industrial Electronics, Faculty of Electronic & Computer Engineering, Universiti Teknikal Malaysia (UTeM) Melaka, Malaysia. His research interests are power electronic controllers for photovoltaic applications, such as inverters and DC–DC converters.